PREDICTION UNDER UNCERTAINTIES

By

Wesley Bowman, Sergei Melkoumian, Nathaniel Richmond, William Thompson, Feifei Wang, Argen West

Mentor: Dr. Albert Gilg

IMA Preprint Series #2436

(September 2014)

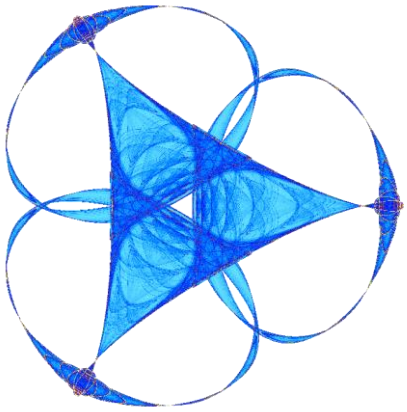

INSTITUTE FOR MATHEMATICS AND ITS APPLICATIONS
UNIVERSITY OF MINNESOTA
400 Lind Hall
207 Church Street S.E.
Minneapolis, Minnesota 55455-0436
Phone: 612-624-6066 Fax: 612-626-7370
URL: http://www.ima.umn.edu

Team 6 Final Report - Prediction Under Uncertainties

Team Members: Wesley Bowman, Sergei Melkoumian, Nathaniel Richmond, William Thompson, Feifei Wang, Argen West

Mentor: Dr. Albert Gilg, Siemens AG & TU Munich

IMA / PIMS Mathematical Modeling in Industry XVIII
August 6-16, 2014

Contents

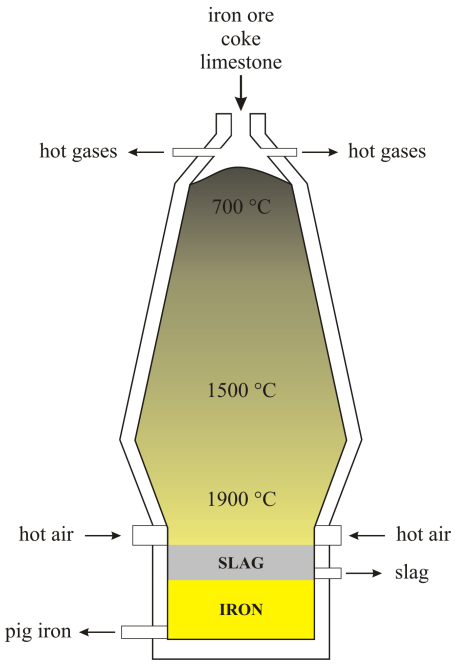

Figure 1: Blast furnace diagram

1 Introduction

Industrial blast furnaces are used for the smelting of ores such as iron, lead, or copper. Due to the high melting points of these metals, extremely high temperatures of around $2000°C$ must be reached, and the furnaces are running for many years without stoppage. Harsh conditions within a blast furnace (See Fig. 1) tend to gradually wear away the interior wall. The high complexity of physical and chemical processes that take place within a blast furnace pose immense challenges in directly computing the shape of the interior wall with knowledge of these processes alone. Instead, it is a common practice in industry to embed thermal sensors within the exterior wall, using these readings to determine when the system has reached a critical point. In this project, we propose a method that takes external sensor data as its input and produces an interior wall shape estimate. We thoroughly examine the efficacy of our method from computational, analytical, and statistical perspectives, especially in the presence of noisy sensor data.

2 The Direct Heat Transfer Problem

In the spirit of targeting the core mathematical problem at hand, we make some simplifying assumptions before introducing the problem at hand.

- *The problem is 2-dimensional.* Even the 2-dimensional problem is a complex problem for reasons we will outline below. However, our results may be generalized and extended to 3 dimensions.
- *The interior temperature of the blast furnace is precisely known.* Determining the temperature of the contents of the bast furnace at any given time is a very challenging task assigned to chemists and physicists. We can expect errors in this data but we ignore them for now.
- *We have exact sensor data.* The thermocouples (heat sensors) placed on the exterior wall are not exact. Typical accuracy ranges for industry thermocouples are within $\pm 0.75\%$ [5]. For the initial problem statement, we assume perfect sensor data. We consider the inherent sensor uncertainty in a later section.
- *The wall between sensors and the interior has homegenous composition.* In practice, there is often some accumulated material on the interior wall in addition to heterogeneities in the composition of the wall. We neglect these effects in our study.

In the blast furnace setting outlined above, the direct heat transfer problem deals with computing the temperature distribution throughout the wall, given the interior temperature and the exact known shape of the wall. It is a safe assumption that the time scale on which the time-dependent heat transfer problem reaches steady state is much shorter than that on which the wall erodes. For this reason, we focus on solving the time-independent heat transfer problem,

$$\Delta u = 0 \tag{2.1}$$

where Δ denotes the Laplacian operator. The associated boundary conditions (BCs) are

$$\begin{cases} \text{Neumann BC on the top (flux free)} & \frac{\partial u}{\partial y}(x, L) = 0 \\ \text{Neumann BC on the bottom (flux free)} & \frac{\partial u}{\partial y}(x, 0) = 0 \\ \text{Dirichlet BC on the inner wall (fixed temp)} & u(w(y), y) = 2000 \\ \text{Robin BC on the outer wall (temp-dependent flux)} & \frac{\partial u}{\partial x}(0, y) = p(u - T_0) \end{cases} \tag{2.2}$$

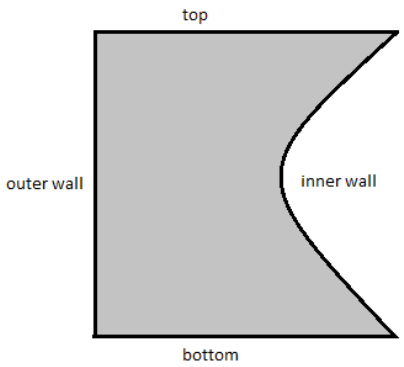

Figure 2: 2D blast furnace wall model

In this system, $u(x, y)$ is the temperature at spatial position (x, y), p is the heat transfer coefficient, T_0 is the ambient exterior temperature, L is the height of the wall, and $w(y)$ defines the thickness of the blast furnace wall at vertical coordinate y. A visual representation of the geometry is given in Fig. 2. We take $(p, T_0) = (1, 25)$.

For modeling simplicity, we assumed Neumann boundary conditions for the top and bottom of the wall. We recognize that this is a physically unrealistic assumption, but believe that other boundary conditions would overcomplicate the model and have little impact on the goals of this project. We assume the interior wall temperature remains fixed at a known level.

3 Solving the Inverse Problem

We are interested in deriving the geometry of the interior wall, given the temperature levels at the interior and exterior walls. This is called the geometric inverse heat transfer problem. Due to the nonlinear interior wall boundary, this problem is difficult to solve analytically. We focus instead on a nonlinear least squares iteration method, which will be introduced next.

As per our boundary conditions (2.2), we suppose the inner wall always has the constant temperature of $2000°\mathrm{C}$. This assumption can be made assuming that a narrow portion of the wall is being investigated. However, any interior temperature profile can be used and we choose this one for simplicity. We put sensors on the outer wall to read the initial temperature profile. As a basic case, we suppose there is only one dent on

the inner wall and use the Gaussian function with parameters h, μ, and σ to describe the dent and the thickness of the wall, w, at position y, as

$$w(y; h, \mu, \sigma) = 1 - h \exp\left(-\frac{(y-\mu)^2}{\sigma^2}\right) \tag{3.1}$$

Here, $\mu \in [0, 1]$ gives the position of the center of the dent, $\sigma > 0$ describes the width of the dent, and $h \in [0, 1)$ represents the depth of the dent in the inner wall. If $h = 0$, there is no dent and the wall has uniform thickness 1.

The estimation process is as follows. We choose some numbers $\mu^{(0)}$, $\sigma^{(0)}$ and $h^{(0)}$ defining our initial estimate of the inner wall shape. Then, we calculate the initial temperature profile of the outer wall by solving the heat equation system (2.1), (2.2) numerically. If the error between the estimated outer wall temperature profile and the sensor data for the outer wall is bigger than a tolerance number, we will use the Levenberg-Marquardt (L-M) nonlinear least squares method to iteratively produce a new set of parameter values for the inner wall. At each iteration, we use the wall shape specified by the current parameters to solve the direct heat equation. We check the error between this output temperature profile and the actual sensor observations until at some iteration step, the error has reached some tolerance level, thus terminating the algorithm.

4 Simulations and Results

We use MATLAB's PDE toolbox to numerically solve (2.1), (2.2) which allows use to define more complicated wall geometries in a straightforward way. Once a solution for the interior temperature profile, $u(x, y)$, is determined for a given set of wall shape parameters, we extract the temperature profile on the outer wall, $u(0, y)$. An example of this is shown in Fig. 3. Unfortunately, this method sometimes produces an error with the message "`No geometry data`" which can be a problem when the nonlinear least squares method is required to generate a solution repeatedly for different parameter values.

To minimize the sum of squares error between the sensor measurements $\underline{\mathbf{u}}$ and the predicted exterior temperature profile $u(0, y_i)$, $i = 1, ..., m$ (where m is the number of sensors), we use MATLAB's `lsqnonlin` command which accepts two key arguments: an vector objective function, $\underline{\mathbf{F}}(\underline{\mathbf{p}})$, and an initial parameter vector guess, $\underline{\mathbf{p}}^{(0)} = [\hat{h}^{(0)}, \hat{\mu}^{(0)}, \hat{\sigma}^{(0)}]^\intercal$. This command minimizes the sum of squares of the entries of $\underline{\mathbf{F}}(\underline{\mathbf{p}})$

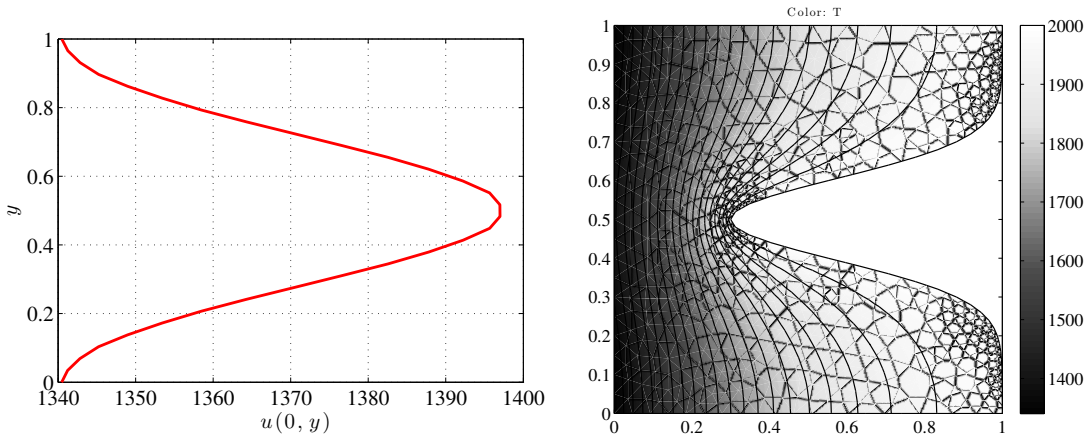

Figure 3: The exterior wall temperature profile (left) for the corresponding cross-sectional wall temperature profile (right) computed by solving the steady state heat equation (2.1) with boundary conditions (2.2). The interior wall shape profile w is given by (3.1) with $(h, \mu, \sigma) = (0.7, 0.5, 0.15)$.

with respect to the entries of $\underline{\mathbf{p}}$. Since we merely want to minimize the sum of squares, the objective function is simply $\underline{\mathbf{F}}(\underline{\mathbf{p}}) = \underline{\mathbf{u}} - \underline{\tilde{\mathbf{u}}}(\underline{\mathbf{p}})$ where $\underline{\mathbf{u}}$ is the set of sensor measurements and $\underline{\tilde{\mathbf{u}}}(\underline{\mathbf{p}})$ is the set of predicted temperatures for a set of parameters $\underline{\mathbf{p}}$ at the sensor locations y_i. We denote our final parameter estimates by $\underline{\hat{\mathbf{p}}}$ and the associated final temperature profile by $\underline{\hat{\mathbf{u}}} = \underline{\tilde{\mathbf{u}}}(\underline{\hat{\mathbf{p}}})$.

In general, our method will obtain estimates that are close to truth in the sense of small relative error and an example of this is shown in Fig. 4. Additionally, we can track changes in the wall structure from a known initial state allowing us to begin the estimation routine from a good initial guess and track changes in the wall structure in time,in principle. However, when the data is noisy, the estimates do not converge so nicely.

4.1 Noisy data

We now consider the more realistic case where the sensor data are noisy. For this consideration we assume that the sensors give data $\underline{\mathbf{u}} = \underline{\dot{\mathbf{u}}} + \underline{\mathbf{e}}$, where $\underline{\dot{\mathbf{u}}}$ is the sensor data without noise as previously discussed and $\underline{\mathbf{e}} \sim \mathcal{N}(\underline{\mathbf{0}}, \zeta^2\mathbf{I})$. We consider a situation identical to that in Fig. 4, but we include some small and "well-behaved" noise. The results are shown in Fig. 5. We observe that while the the temperature profile is well-estimated, the wall profile is not-so-well estimated. This example highlights the ill-posedness of

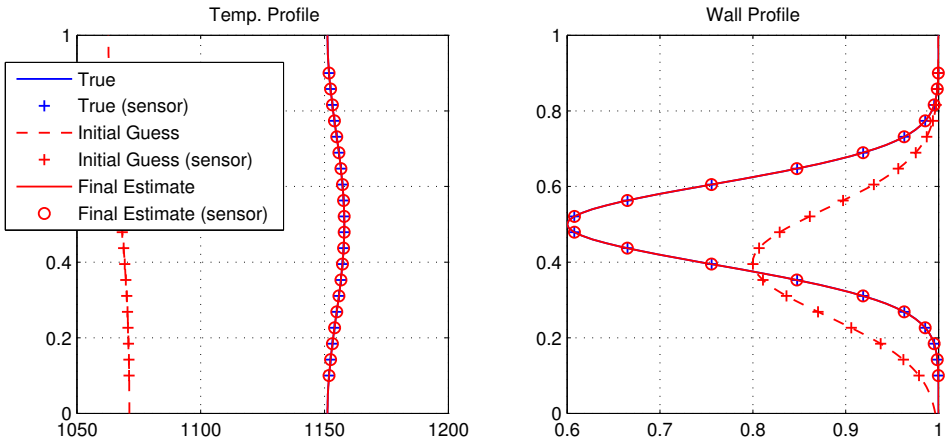

Figure 4: An example estimate of the inner wall profile for perfectly measured data with wall parameters $\underline{\mathbf{p}} = [0.4,\, 0.5,\, 0.15]^\intercal$. The relative error in each final parameter estimate is given by $[0.1505,\, 0.0004,\, -0.8818]^\intercal \times 10^{-3}$. The initial parameter "guesses" were $\underline{\mathbf{p}}^{(0)} = [0.2,\, 0.4,\, 0.2]^\intercal$. The positions of the 20 sensors are indicated with crosses and circles as the legend describes.

the inverse heat problem in that similar temperature profiles result from very different parameter values.

5 Statistical Perspectives

Having obtained the parameter estimates $\hat{\underline{\mathbf{p}}} = [\hat{h}, \hat{\mu}, \hat{\sigma}]^\intercal$ using the L-M method, we would like to understand and provide a quality measure of these results in terms of confidence intervals (CIs). For m sensor measurements, we have an $m \times m$ diagonal weighting matrix $\mathbf{W}$ with diagonal components $W_{ii} = 1/S^2$ where S^2 is an estimator of the sample variance in the data $\underline{\mathbf{u}}$ given model temperatures $\hat{\underline{\mathbf{u}}}$ corresponding to the estimated parameters $\hat{\underline{\mathbf{p}}}$,

$$S^2 = \frac{1}{m-n+1}(\underline{\mathbf{u}} - \hat{\underline{\mathbf{u}}})^\intercal(\underline{\mathbf{u}} - \hat{\underline{\mathbf{u}}}) \tag{5.1}$$

and $n = 3$ is the number of parameters (h, μ and σ). The standard deviation of the parameters is defined by

$$\underline{\boldsymbol{\Sigma}}_{\underline{\mathbf{p}}} = \sqrt{\mathrm{diag}\left((\mathbf{J}^\intercal\mathbf{W}\mathbf{J})^{-1}\right)} = |S|\sqrt{\mathrm{diag}\left((\mathbf{J}^\intercal\mathbf{J})^{-1}\right)} \tag{5.2}$$

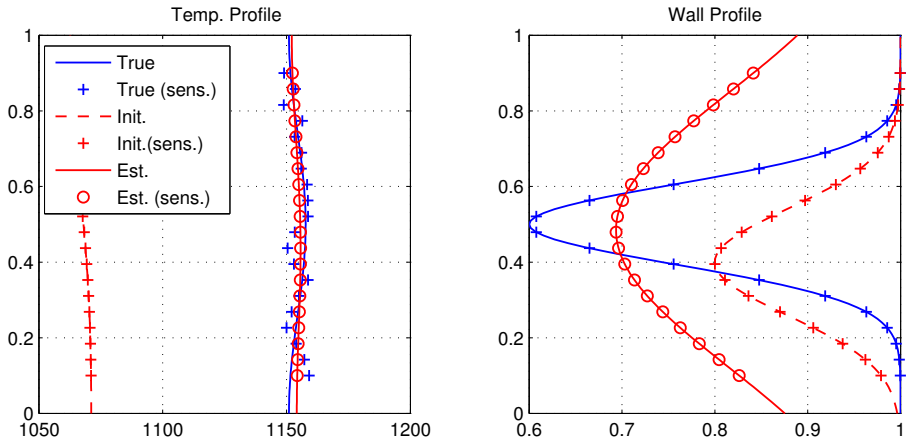

Figure 5: An example estimate of the inner wall profile for noisy data with wall parameters $\underline{\mathbf{p}} = [0.4,\ 0.5,\ 0.15]^\intercal$. Each sensor measurement is perturbed by normally distributed noise with mean zero and variance $\zeta^2 = 3^2$. The final parameter estimates were $\hat{\underline{\mathbf{p}}} = [0.3064, 0.4850, 0.5113]^\intercal$.

where $\mathbf{J} = [\partial\hat{\underline{\mathbf{u}}}/\partial\underline{\mathbf{p}}]$ is a $m\times n$ Jacobian matrix at the final iteration of the L-M method:

$$\mathbf{J} = \nabla\hat{\underline{\mathbf{u}}}(\hat{\underline{\mathbf{p}}}) = \begin{bmatrix} \frac{\partial}{\partial h}\hat{u}_1(\hat{\underline{\mathbf{p}}}) & \frac{\partial}{\partial \mu}\hat{u}_1(\hat{\underline{\mathbf{p}}}) & \frac{\partial}{\partial \sigma}\hat{u}_1(\hat{\underline{\mathbf{p}}}) \\ \frac{\partial}{\partial h}\hat{u}_2(\hat{\underline{\mathbf{p}}}) & \frac{\partial}{\partial \mu}\hat{u}_2(\hat{\underline{\mathbf{p}}}) & \frac{\partial}{\partial \sigma}\hat{u}_2(\hat{\underline{\mathbf{p}}}) \\ \vdots & \vdots & \vdots \\ \frac{\partial}{\partial h}\hat{u}_m(\hat{\underline{\mathbf{p}}}) & \frac{\partial}{\partial \mu}\hat{u}_m(\hat{\underline{\mathbf{p}}}) & \frac{\partial}{\partial \sigma}\hat{u}_m(\hat{\underline{\mathbf{p}}}) \end{bmatrix}, \quad \hat{u}_i = \hat{u}(0, y_i). \tag{5.3}$$

The matrix $\mathbf{J}^\intercal\mathbf{J}$ gives a linearized quantification of the sensitivity of the temperature at each sensor location to small perturbations in the parameters. $\underline{\mathbf{\Sigma}}_{\underline{\mathbf{p}}}$ is a 3×1 vector and contains the standard deviation of each parameter as its elements. Thus for $\alpha \in (0, 1)$ we can compute the $(1-\alpha)\times 100$ % CI of each parameter by taking $\hat{\underline{\mathbf{p}}} \pm z(\alpha)\underline{\mathbf{\Sigma}}_{\underline{\mathbf{p}}}$ where $z(\alpha)$ is the corresponding z-score for the $(1-\alpha)\times 100\%$ CI. For the remainder of the paper we consider the 99% CI and take $\alpha = 0.01$ (i.e. $z(\alpha) = 2.5758$).

Additionally, we use some theory from principal components analysis (PCA) to determine the primary modes of variability in our parameter estimates by computing the eigenstructure of the estimated covariance matrix, $S^2(\mathbf{J}^\intercal\mathbf{J})^{-1}$. The eigenvectors with the largest corresponding eigenvalues give the primary modes of variability.

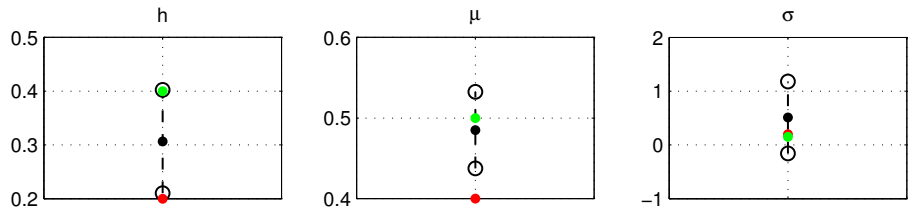

Figure 6: The 99% CIs on each parameter for the situation outlined in Fig. 5. The initial and final parameter estimates are marked by the red and black dots resp. while the true value is marked in green.

5.1 A moderately deep, narrow dent

Considering the example discussed in Section 4.1, we place a CI on the parameter estimates that were obtained. Using the theory outlined in the previous section, we compute the 99% CIs on h, μ and σ, and display the results in Fig. 6. As a basic check for consistency, we see the true values of the parameters all lie within the 99% CIs surrounding the parameter estimates, $\underline{\hat{\mathbf{p}}}$. Using PCA, we determine numerical estimates for the eigenvalues of the estimated covariance matrix $S^2(\mathbf{J}^\intercal\mathbf{J})^{-1}$: $\underline{\hat{\lambda}} = [0.0689,\ 0.0003,\ 0.0000]^\intercal$. Thus, the first eigenmode contains the most variability by far. The corresponding eigenvector is $\underline{\hat{\mathbf{v}}_\mathbf{1}} = [-0.1421,\ -0.0292,\ 0.9894]^\intercal$ where the entries of $\underline{\hat{\mathbf{v}}_\mathbf{1}}$ correspond to variation in h, μ and σ resp. This indicates that the greatest variability in parameter estimates occurs locally along a direction where estimates of h and σ are negatively correlated.

5.2 A deeper, wider, off-centre dent

We consider another example of wall shape estimation where the true shape of the wall is defined by the parameters $\underline{\mathbf{p}} = [0.7,\ 0.6,\ 0.2]^\intercal$ and the temperature data is subject to noisy perturbations that are normally distributed with mean zero and variance $\zeta^2 = 8^2$. By the results in Fig. 7, we see that the estimation method is successful, giving parameters that are close to truth: $\underline{\hat{\mathbf{p}}} = [0.6959,\ 0.6054,\ 0.2179]^\intercal$. Moreover, the true parameters are contained well within the 99% CIs.

By PCA, the leading order mode of the covariance matrix has eigenvalue which is $\simeq 100$ times larger than the next largest eigenvalue. The corresponding eigenvector is given by $\underline{\hat{\mathbf{v}}_\mathbf{1}} = [-0.2203,\ 0.1322,\ 0.9664]^\intercal$, once again indicating that the variability

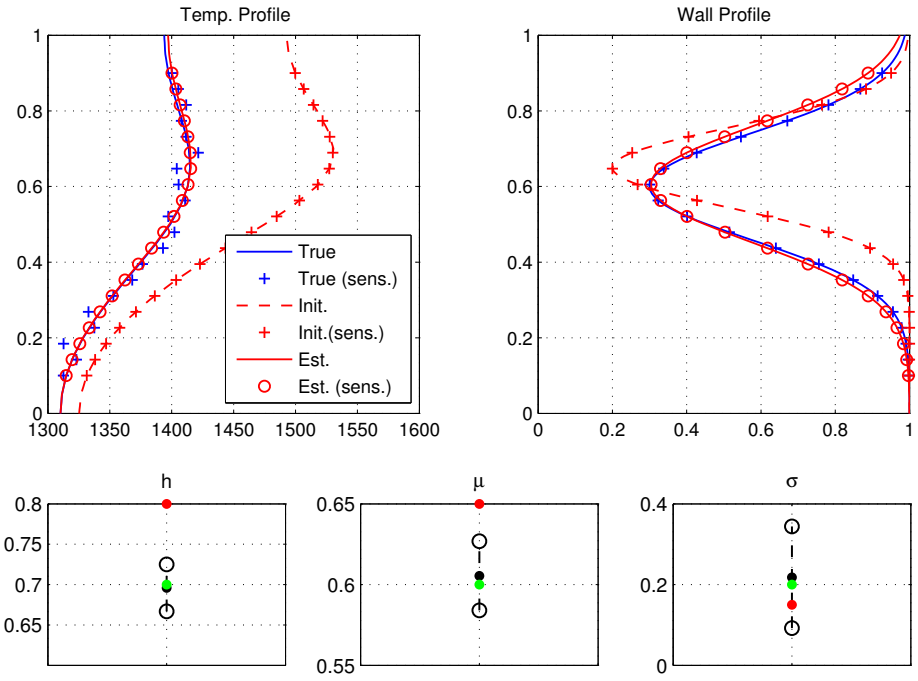

Figure 7: Top: The exterior temperature profiles (left) and corresponding wall profiles for the true parameters, the initial guess and the final estimates of the parameters. Bottom: The 99% CIs on each parameter. The initial and final parameter estimates are marked by the red and black dots resp. while the true value is marked in green. The true values are well within the 99% CI.

in the parameter estimates occurs along a direction in which h and σ are negatively correlated.

6 Further Investigations

There are many potential questions that could be investigated using the simulation test bed that we have created and we include two interesting investigations that could be directly addressed.

6.1 Positioning of sensors

To see how positioning of sensors may have an effect on the quality of parameter estimates we conduct an experiment where we position a fixed number of sensors in

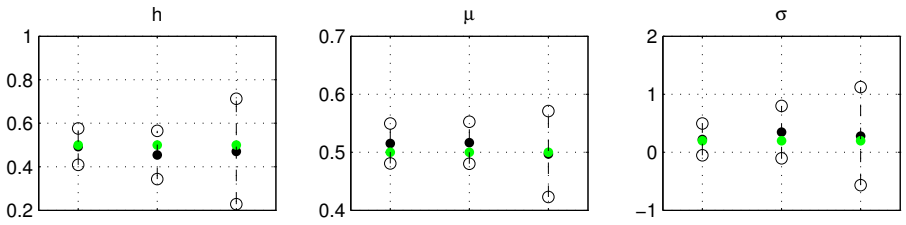

Figure 8: 99% CIs for the parameters h, μ, and σ. In each plot from left to right, the sensors ($m = 20$) are placed with uniform spacing on $[0.1,\ 0.9]$, $[0.1,\ 0.3] \cup [0.7,\ 0.9]$, and $[0.3,\ 0.7]$. The true (estimated) parameter values are indicated with green (black) dots. The initial guess for the parameter estimates is equal to the true parameters.

different arrangements to see the effect on the confidence intervals. We consider three different arrangements: uniformly spaced sensors on the entire wall, uniformly spaced sensors away from the centre of the wall and uniformly spaced sensors near the centre of the wall. The dent in the wall has parameters $\underline{\mathbf{p}} = [0.5,\ 0.5,\ 0.2]^\intercal$ and the temperature measurements have normal errors with variance $\zeta^2 = 8^2$. From the results displayed in Fig. 8, we see that uniform spacing of sensors in this situation is the best option as it gives the smallest confidence intervals. Placing sensors near the edges gives similar results, but localizing sensors over the dent gives wider confidence intervals. This result may be contrary to intuition as one might think that having sensors located near a wall anomaly would lead to more accurate detection of the anomaly, but these results invalidate this hypothesis. This surprising result may be justified by the suggestion that a uniform placement of sensors along the outer wall provides us with a complete set of data for the entire wall, which may be more valuable than high concentrations of data on a restricted portion of the wall. In the extreme case, one could think of placing all sensors at one particular point, which would give accurate local information but disregards anything else about how the temperature profile changes with position. Additionally, localizing sensors around a particular region does not make sense as an engineering choice as placing sensors in one area implies the expectation that a breach will happen within that area. Uniform placement makes the most sense from an operational point of view as you do not expect a breach to occur at any one point along the wall.

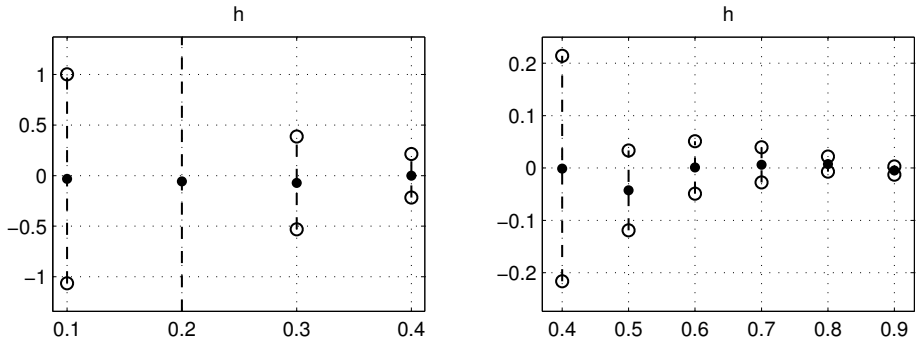

Figure 9: 99% CIs for the parameter h, minus the true value of h. The horizontal axis indicates the true value of h. The true values of $(\mu, \sigma) = (0.5, 0.2)$. The initial guess for parameters at each value of h were set to be the estimates obtained at $h - 0.1$, with the initial guess at $h = 0.1$ given by $\underline{\mathbf{p}}^{(0)} = [0.05, 0.45, 0.25]^\intercal$. The data were subject to normally distributed noise with variance equal to $0.5\%\hat{\underline{\mathbf{u}}}$. The confidence interval for the $h = 0.2$ case has radius $\simeq 10$.

6.2 Width of CIs and the depth of the dent

The parameter h is of paramount importance for blast furnace operation. Under our assumption of a Gaussian-shaped dent, h defines the depth of the dent in the wall. As $h \to 1^-$, the wall comes closer to failing. To address the question of how the certainty of the parameter estimates is affected as h increases, we compute the confidence intervals for increasing values of h. We first assume a relatively shallow dent exists and estimate the shape of the walls. Once an estimate is achieved, we increase h to $h + 0.1$ and use the previous parameter estimates as the initial guess for the following estimate. We assume the strength of the noise in the data is proportional to the temperature being measured in accordance with [5]. The results are shown in Fig. 9. The results indicate that the uncertainty in the parameter h decreases as $h \to 1^-$. This is a positive result for furnace operators since as the wall becomes thinner, it becomes easier to determine how thin the wall is. The CIs of μ, σ show similar behaviour to those of h, indicating that the location and scope of the breach can be more accurately estimated as h increases to 1.

7 Conclusions and Extensions

In this project, we implemented a method of parameter estimation to predict the thickness of a blast furnace wall under simple assumptions of the form of the indentation (i.e. the Gaussian dent). The assumptions used in our study regarding the physical problem were throughly checked and listed. Future work may investigate the validity of critical assumptions used here. When the data are perfect, the nonlinear least squares method we apply to estimate the geometry of the wall is robust and predicts the wall geometry with a high degree of accuracy. When noise is included in the measurements, the ill-posedness of the problem becomes apparent and there is a set of geometries that could conceivably give the measurements observed (i.e. a thin narrow dent and a fat wide dent return similar temperature profiles). Given this uncertainty, we apply a linear analysis to determine confidence intervals on parameter estimates, which typically contain the true parameter values under 99% confidence. We observe that the confidence tend to be more narrow when the sensors are uniformly spaced along entire wall, rather than concentrated at specific locations. Using this result, we uniformly place sensors along the entire wall to determine how the confidence intervals vary in response to different indentation depths. As the depth of the dent increases, the confidence intervals tend to become more narrow, indicating that greater certainty about the thickness of the wall is obtained as the wall comes closer to failing.

While our study has been a success, there are some ways that the results can be improved. Our use of the MATLAB PDE toolbox was for expediency and the fact that complicated geometries can be handled with ease. Unfortunately, computational errors and exceptions (i.e. "`no geometry data`") hindered the study and we were limited to studying problems in certain parameter regimes, such as $\sigma > 0$, not too small. For continuing study, a more robust method for solving the heat problem (2.1), (2.2) would be advantageous.

There are several ways that this work could be extended for more insight into the problem of uncertainty in geometric inverse heat transfer problems. A relatively simple extension would be to consider interior wall profiles which are given by a sum of Gaussian-shaped dents. This would allow for more "exotic" wall profiles. Additionally, one could also consider an inner wall profile composed of piecewise linear functions or cubic splines. A more involved study could consider the extension of our results to 3-dimensional geometries, but this would likely require some heavy-duty computation.

A topic we would like to explore in more detail is optimal operation via stochastic optimization. An industrial operator of a blast furnace wishes to plan operation of the furnace for the future, based on the current data. Our work in this project presents a valid method for producing an optimal estimate for the interior wall, together with confidence intervals on the associated parameters. As any changes in the interior wall depend solely on the current state and the operational load placed on it, we may naturally model the operational strategy problem as a Markov Decision Process. The parameter values and confidence intervals obtained from our method may be chosen to represent the *state* of the system. Historical operational data may be used to produce the *transition probability matrix*, and the operator has at his/her disposal a set of relevant *actions*. By using a Markov Decision Process model, one can simulate the likely transformation of the interior wall over time, in response to the operator's choices. The solution of this Markov Decision Process model would produce an optimal solution function which prescribes which actions to take for different states of the system. Such a model could serve as a guide to industrial blast furnace operators.

8 Acknowledgements

All the participants acknowledge and extend their thanks to the Pacific Institute for the Mathematical Sciences (PIMS) and the Institute for Mathematics and its Applications (IMA) for organizing the workshop. They would also like to thank the University of British Columbia for their hospitality. The team members would also like to thank their mentor Dr. Albert Gilg for his advice and input to the project over the duration of the workshop.

References

[1] http://galleryhip.com/blast-furnace.html

[2] Flynn, D., Nalco Water Handbook, 3rd Ed. The Steel Industry, Chapter (McGraw-Hill Professional, 2009), AccessEngineering
http://accessengineeringlibrary.com/browse/nalco-water-handbook-third-edition/p2001875199737_1001

[3] Gavin, H. (2013). *The Levenberg-Marquardt method for nonlinear least squares curve-fitting problems*.
http://people.duke.edu/~hpgavin/ce281/lm.pdf.

[4] Swartling, M. (2010). *A Study of the Heat Flow in the Blast Furnace Hearth Lining*. Royal Institute of Technology, Stockholm, Sweden.
http://www.diva-portal.org/smash/get/diva2:321371/FULLTEXT02

[5] http://www.thermocoupleinfo.com